REFERENCES
Amils, R., Matthews, E., & Cantor, C. (1979) *Methods Enzymol. 59*, 449–461.
Bayley, S. T. (1966a) *J. Mol. Biol. 18*, 330–338.
Bayley, S. T. (1966b) *J. Mol. Biol. 15*, 420–427.
Bayley, S. T., & Kushner, D. J. (1964) *J. Mol. Biol. 9*, 654–669.
Fahnestock, S. (1979) *Methods Enzymol. 59*, 437–443.
Londei, P., Teixido, J., Acca, M., Cammarano, P., & Amils, R. (1986) *Nucleic Acids Res. 14*, 2269–2285.
Makowski, I., Frolow, F., Saper, M. A., Wittman, H. G., & Yonath, A. (1987) *J. Mol. Biol. 193*, 819–827.
Mans, R. J., & Novelli, G. D. (1961) *Arch. Biochem. Biophys. 94*, 48–53.
Nierhaus, K. H., & Dohme, F. (1974) *Proc. Natl. Acad. Sci. U.S.A. 71*, 4713–4717.
Nierhaus, K. H., & Dohme, F. (1979) *Methods Enzymol. 59*, 443–449.
Rodriguez-Valera, F., Juez, G., & Kushner, D. J. (1983) *Syst. Appl. Microbiol. 4*, 369–381.
Sanz, J. L., Marin, I., Balboa, M. A., Ureña, D., & Amils, R. (1988) *Biochemistry 27*, 8194–8199.
Schulze, H., & Nierhaus, K. H. (1982) *EMBO J. 1*, 609–613.
Strom, A. R., & Visentin, L. P. (1973) *FEBS Lett. 37*, 274–280.
Strom, A. R., Hasnain, S., Smith, N., Matheson, A. T., & Visentin, L. P. (1975) *Biochim. Biophys. Acta 383*, 325–337.
Torreblanca, M., Rodriguez-Valera, F., Juez, G., Ventosa, A., Kamekura, M., & Kates, M. (1986) *Syst. Appl. Microbiol. 8*, 89–99.
Visentin, L. P., Chow, C., Matheson, A. T., Yaguchi, M., & Rollin, F. (1972) *Biochem. J. 130*, 103–110.
Yonath, A., Leonard, K. R., & Wittman, H. G. (1987) *Science 236*, 813–816.

Analysis of Fluorescence Energy Transfer in Duplex and Branched DNA Molecules†

Julia Promisel Cooper and Paul J. Hagerman*
Department of Biochemistry, Biophysics and Genetics, B-121, University of Colorado Health Sciences Center, 4200 East Ninth Avenue, Denver, Colorado 80262
Received April 19, 1990; Revised Manuscript Received July 3, 1990

ABSTRACT: Nonradiative fluorescence energy transfer (FET) is thought to be a highly sensitive measure of distance, occurring through a dipole coupling (Forster) mechanism in which the efficiency of FET depends on the inverse sixth power of the distance between fluorophores. The current work assesses the utility of FET for measuring distances in duplex and branched DNA molecules. The apparent efficiencies of FET between donor (fluorescein) and acceptor (eosin) fluorophores attached to opposite ends of oligonucleotide duplexes of varying length were determined; the results suggest that FET is a useful qualitative indicator of distance in DNA molecules. However, the apparent FET efficiency values cannot be fit to the Forster equation without the specification of highly extended DNA-to-fluorophore tethers and motionally restricted fluorophores, conditions that are unlikely to coexist. Three other lines of evidence further suggest that factors in addition to Forster transfer contribute to apparent FET in DNA: (1) The efficiency of FET appears to depend on the base sequence in some instances. (2) Donor fluorescence changes with the extent of thermally induced DNA melting in a sequence-dependent fashion, indicating dye–DNA interactions. (3) The distances between the ends of various pairwise combinations of arms of a DNA four-way junction do not vary as much as expected from previous work. Thus, the occurrence of any nondipolar effects on energy transfer in oligonucleotide systems must be defined before distances in DNA molecules can be quantified by using FET.

The characterization of DNA structure often requires techniques for measuring distances between particular sites on DNA molecules in free solution. Such techniques can, in principle, provide information on the geometries of bent or branched DNA molecules, thus enabling the interpretation of results obtained from studies of the same molecules in constrained environments (e.g., in gels or crystals). The present report describes a preliminary assessment of the utility of fluorescence energy transfer (FET) for measuring the distances between the ends of oligonucleotide duplexes and branched structures in solution.

Our initial motivation for pursuing FET studies of oligonucleotides stemmed from our work on the structure of a synthetic DNA four-way junction (Cooper & Hagerman, 1987, 1989), in which gel electrophoretic and hydrodynamic analyses were utilized. While the limitations of the gel method (Cooper & Hagerman, 1987) were largely overcome by the determination of rotational diffusion times (Cooper & Hagerman, 1989), both methods require the attachment of reporter fragments to specified arms of the junction, followed by several purification steps. Thus, we sought a method for measuring junction interarm angles that would be performed in free solution and that would obviate the need for attachment of reporter fragments. The distance range that is considered accessible to FET (~10–90 Å) should, in principle, allow evaluation of the magnitudes of the junction interarm angles

† This research was supported by Grant GM35305 from the National Institutes of Health.
* Author to whom correspondence should be addressed.

0006-2960/90/0429-9261$02.50/0

by measuring FET between donor and acceptor fluorophores at the ends of junction arms. Several additional features of FET would appear to make it an attractive method for studying small synthetic DNA structures. FET measurements can be performed under a wide variety of conditions (e.g., low- and high-salt buffers) and at relatively low DNA concentrations. Furthermore, FET is considered a highly sensitive measure of distance; in particular, FET is thought to occur through the dipole-coupling mechanism proposed by Forster (1948), in which the efficiency (E) of FET depends on the inverse sixth power of the distance (R) between donor and acceptor fluorophores.

The R^{-6} dependence of E was verified experimentally by Stryer and Haugland (1967) for a series of oligo-L-proline molecules of varying length. FET has since been used to measure distances in tRNA and rRNA molecules (Beardsley & Cantor, 1970; Yang & Soll, 1974; Odom et al., 1980; Robbins et al., 1981); and recently, exploratory attempts have been made in oligonucleotide systems (Cardullo et al., 1988; Murchie et al., 1989). However, the applicability of Forster's theory to nucleic acid systems has not yet been explicitly demonstrated. The recent advent of rapid oligonucleotide synthesis has afforded a straightforward approach to test the validity of the Forster mechanism in DNA molecules. In particular, fluorescent probes can be attached to oligonucleotides via aliphatic primary amino groups that are themselves specifically linked to the 5′-ends of DNA molecules (Smith et al., 1985). Thus, the goals of the current work were (1) to measure FET between fluorophores attached to the ends of oligonucleotide duplexes of varying length, in order to establish the length dependence of FET in DNA, and (2) to use FET to determine the distances between the ends of the arms of a DNA four-way junction. Two conclusions can be drawn from this study. First, FET provides a useful qualitative tool for measuring distances in DNA, although the Forster equation does not account quantitatively for the observed range of transfer efficiencies. Second, although the relative junction interarm angles obtained from FET measurements agree qualitatively with those derived from gel electrophoretic and hydrodynamic studies, the possibility of alternative pathways for energy transfer precludes the quantitation of interarm angles by FET.

Materials and Methods

Synthesis and Purification of 5′-Amino Oligonucleotides. In order to effect the specific attachment of fluorescent dyes to the 5′-ends of oligodeoxyribonucleotides, a primary amino group was linked to the 5′-end of each oligonucleotide by using the phosphoramidite, aminolink 1 (Applied Biosystems). Oligonucleotides were synthesized on controlled pore glass (CPG) supports, using a Biosearch Model 8750 automated DNA synthesizer. Standard phosphoramidite chemistry (Caruthers et al., 1982; Atkinson & Smith, 1984) was employed, with a modified final cycle for aminolink addition, as specified by Biosearch. Cleavage of DNA from CPG supports, base deprotection, and oligonucleotide purification were carried out as described by Hagerman (1985). The resulting molecules possessed a primary amino group, attached through an aliphatic (two-carbon) chain and a phosphodiester linkage to the 5′-carbon of the deoxyribose.

The sequences of the oligonucleotide duplexes synthesized for the FET experiments are listed in Table I. For FET studies of a synthetic DNA four-way junction, a shortened version of the junction described previously (Cooper & Hagerman, 1987, 1989) was produced, in order to ensure that the distances between the ends of junction arms would fall within the range accessible to FET measurements. The sequences of the strands comprising the junction are listed in Table I and are related to those comprising the 30-mer junction employed previously by the deletion of seven bases from the 5′-end of each 30-mer, the deletion of three bases from the 3′-end of each 30-mer, and the addition of a thymidine residue to the 5′-end of the resulting sequences. Each arm of the annealed four-way junction therefore contains 10 paired bases and a 5′-thymidine overhang.

Table I. Sequences of Oligonucleotides for FET Measurements

species	sequence[a]
7-mer	5′TGAGCAT
9-mer(a)	5′TGAGGCCAT
9-mer(b)	5′TACGAGCGT
11-mer	5′TGAAGGCCGAT
13-mer	5′TGATAGGCCGTAT
15-mer	5′TGATTAGGCCGTTAT
20-mer	5′TACGAGCGTAGATGCGAGCT
21-mer	5′TCGGCTCTCGGACTAGTCCCG
junction strand 1	5′TATCGACGTCACCGAGAGCCG
junction strand 2	5′TGCTGGAATCCTGACGTCGAT
junction strand 3	5′TCGGGACTAGTGGATTCCAGC
junction strand 4	5′TCGGCTCTCGGACTAGTCCCG

[a] Sequence of donor-linked strand; each duplex, referred to as "n-mer", consists of $n - 1$ paired bases with a 5′-T overhang at each end, for example, the 7-mer has the following sequence:

5′-TGAGCAT
CTCGTAT-5′

Conjugation of Fluorophores to 5′-Amino Oligonucleotides. Dye conjugation reactions were carried out essentially as described by Smith et al. (1985): 5′-amino oligonucleotides were incubated with a 400-fold molar excess of fluorophore in 200 mM sodium carbonate/bicarbonate (pH 9.0) for several hours in the dark, at room temperature. Fluorophores, obtained from Molecular Probes, Inc., and stored desiccated at −20 °C, were dissolved in dimethylformamide immediately prior to their reaction with the 5′-amino oligomers. Free dye was removed from the dye-linked oligonucleotides by two rounds of ethanol precipitation (80% v/v ethanol, 0.3 M potassium acetate). Dye-linked oligonucleotides were resuspended in 0.1 M triethylammonium acetate prior to high-pressure liquid chromatography (HPLC).

Purification of Fluorophore-Linked Oligonucleotides by HPLC. Dye-linked oligonucleotides were separated from their unlabeled counterparts by reverse-phase HPLC, using either a Gilson gradient programmer and solvent delivery system or Beckman 110B pumps run by System Gold (Beckman) software, equipped with an online ultraviolet absorbance detector. Radial-PAK C18 cartridges (Waters), preceded by C18 guard columns, were employed for the separations, using linear gradients of increasing acetonitrile/0.1 M triethylammonium acetate, pH 7.0. Fractions containing fluorophore-linked DNA were identified by measurements of both fluorescence and ultraviolet absorbance. Dye-linked DNA was recovered by lyophilization of the appropriate peak fractions and was resuspended in 10 mM Tris-HCl, pH 8.0, and stored in the dark at −70 °C.

Absorbance Measurements. DNA concentrations were determined by ultraviolet light absorbance on a Cary 219 spectrophotometer, using the relationship $A_{260} = 28.5$ for a 1 mg/mL solution of single-stranded DNA. Since the ex-

tinction coefficients of dye-linked oligonucleotides were not determined, the above relationship represents an estimate in the latter instance. Therefore, the relative amounts of donor- and acceptor-linked oligonucleotide required to produce samples containing a molar excess of acceptor-linked strand were determined empirically (see Results and Discussion), and concentrations specified in figure and table legends are approximate. Thermal denaturation studies were performed on the Cary 219 spectrophotometer with an indwelling temperature probe in an adjacent cell, using a Lauda circulating bath to raise the temperature (at a rate of less than 0.3 deg/min).

Fluorescence Measurements. Fluorescence measurements were performed on an SLM-AMINCO 48000S spectrofluorometer (kindly made available by Dr. Charles McHenry) equipped with a 450-W xenon arc lamp, monochromators with holographic gratings, cooled photomultiplier tube housings, and a Lauda RM6 water bath for temperature control. The 48000 program was run by an IBM PC/AT. The excitation wavelengths used for fluorescein, eosin, and tetramethylrhodamine were 496, 528, and 552 nm, respectively (excitation band-pass 1 nm). For excitation spectra, the emission wavelengths used were 518 nm for fluorescein, 547 nm for eosin, and 578 nm for tetramethylrhodamine (emission band-pass 4 nm). The optical densities at the excitation wavelength were maintained below 0.03 for all samples to ensure that inner filter effects were negligible. Unless otherwise specified, the cell temperature was maintained at 4.5–5.5 °C.

Determination of R_0. For Forster FET, distances (in Å) between donor and acceptor fluorophores are deduced from the relationship

$$R = R_0[(1 - E)/E]^{1/6}$$

R_0 is the critical transfer distance at which $E = 0.5$, calculated from

$$R_0 = 9786(J\kappa^2 n^{-4} Q_D)^{1/6}$$

where κ^2 is a factor characterizing the relative orientations of donor and acceptor fluorophores, n is the refractive index of the medium, Q_D is the quantum yield of the donor, and J is the spectral overlap integral

$$J = \int \epsilon_A(\lambda) f_D(\lambda) \lambda^4 \, d\lambda / \int f_D(\lambda) \, d\lambda$$

J was calculated from the absorption spectrum of a 13-mer duplex possessing an eosin acceptor, but no donor (referred to as AU; see Results and Discussion), and the fluorescence emission spectrum of a 13-mer duplex possessing a fluorescein donor, but no acceptor (referred to as DU; see Results and Discussion). The extinction coefficient of free eosin isothiocyanate (83 000 at 522 nm, Molecular Probes Handbook) was used as ϵ_A (522 nm). Comparison of the absorbance of a given quantity of free eosin isothiocyanate with that of the same quantity of eosin conjugated to an oligonucleotide suggested that the extinction coefficient may decrease by up to 10% upon attachment to DNA. However, a decrease in ϵ_A of 10% would lead to only a 2% decrease in R_0.

The value of $Q_D = 0.45$ was derived by comparing the absorbance and emission of a 13-mer DU sample with that of a standard solution of known quantum yield (disodium fluorescein in 0.1 N NaOH, $Q_D = 0.92$; Weber & Teale, 1957). The refractive index was taken to be 1.4. If a κ^2 value of two-thirds is assumed (implying unlimited orientational freedom of both donor and acceptor transition dipoles), the resulting value for R_0 is 55 Å, in reasonable agreement with previously published values (Odom et al., 1980; Taylor et al., 1981; Robbins et al., 1981; Holowka & Baird, 1983a,b). The actual range of possible κ^2 values is discussed below (Results and Discussion).

Polarization Measurements. Steady-state polarization measurements were performed on the SLM-AMINCO 48000S with Glan-Thompson polarizers, Schott OG-515 cutoff filters for fluorescein, and KV-550 cutoff filters for eosin. Polarization (P) and anisotropy (A) were calculated by using the SLM single point polarization program, which carries out the following operations:

$$P = (F_v - F_h)/(F_v + F_h)$$

and

$$A = 2P/(3 - P)$$

where F_v and F_h are the fluorescence intensities measured with the excitation polarizer in the vertical and horizontal positions, respectively. Polarization measurements were performed on samples containing varying concentrations of glycerol at 20 °C or sucrose at 5 °C, and depolarization factors were derived from the resulting Perrin plots (Fairclough & Cantor, 1978). The procedure described by Dale et al. (1979) was used subsequently to define the limits of κ^2.

Analysis of Variance. In order to establish whether the variation among sample means was greater than it should be due to chance, variance ratios (F) were determined for various theoretical Forster curves:

$$F = (\mathrm{RMS})^2/[(n - 1)(S_T^2)]$$

where RMS equals the root mean squared difference between the experimental points and a given Forster curve, n equals the number of experimental points (i.e., the number of molecules in the experimental set), and

$$S_T^2 = \sum_i [S_i(E_{app})]^2 (m_i - 1)/[(\sum_i m_i) - n]$$

where $S(E_{app})$ equals the sample standard deviation of E_{app} (apparent transfer efficency) associated with a given molecule and m_i equals the number of E_{app} determinations for a given molecule (i). Levels of significance were derived from F values using F distribution tables (Merrington & Thompson, 1943).

Results and Discussion

Specific Labeling of 5′-Amino Oligonucleotides with Fluorescent Probes. The accurate interpretation of FET data requires the use of DNA molecules that are uniformly labeled at their 5′-ends. In the present study, production of DNA for FET experiments utilized gel-purified 5′-amino oligonucleotides, in order to avoid labeling any failure sequences that might contain the 5′-amino group. For a given oligonucleotide, the success of a dye conjugation reaction was confirmed by the appearance on polyacrylamide gels of a single fluorescent band with an electrophoretic mobility slightly slower than that of the unlabeled 5′-amino oligonucleotide. When oligonucleotides lacking the 5′-amino group were subjected to the dye conjugation procedure, no such fluorescent bands were detectable. Optical densities at the wavelength of maximum fluorophore absorption were zero for the molecules lacking the 5′-amino group, thus providing further verification that only the 5′-amino oligonucleotides were derivatized. Thus, fluorescent labeling of the oligonucleotides occurs uniquely at the 5′-amino site with little or no nonspecific labeling.

Stability of the Oligonucleotide Duplexes and Junction Used for FET Experiments. The arms of the DNA four-way junction employed previously (Cooper & Hagerman, 1987, 1989) were shortened for the current FET studies (see Ma-

Table II: Melting Behavior of Oligonucleotide Duplexes and the DNA Four-Way Junction

species	solution composition[a]	T_0[b] (°C)	T_m[c] (°C)
7-mer	40 mM Tris acetate, 20 mM sodium acetate, 1 mM NaEDTA, 5 mM magnesium acetate, pH 7.9	8	21
9-mer	40 mM Tris acetate, 20 mM sodium acetate, 1 mM NaEDTA, 5 mM magnesium acetate, pH 7.9	10	38
11-mer	10 mM Tris-HCl, pH 8.0	10	25.5
11-mer	20 mM Tris-HCl, 50 mM NaCl, 1 mM EDTA, pH 8.0	15	40
11-mer	10 mM Tris-HCl, 5 mM $MgCl_2$, pH 8.0	20	45.5
11-mer	50 mM Tris-HCl, 10 mM $MgCl_2$, 50 mM NaCl, pH 8.0	20	48
10 bp/arm junction	10 mM Tris-HCl, 5 mM $MgCl_2$, pH 8.0	25	49
10 bp/arm junction	40 mM Tris acetate, 20 mM sodium acetate, 1 mM EDTA, pH 7.9	10	27.5

[a] Total DNA concentrations were approximately 5 μg/mL for all samples; all strands were unlabeled. [b] Highest temperature at which the percent denaturation, as measured by hyperchromic change at 260 nm, is less than 1%; points were recorded on melting curves every 5 deg. [c] Temperature at which the percent hyperchromicity associated with the thermal transition is equal to 50%.

terials and Methods). To ascertain the stability of this smaller junction, as well as of the short duplexes used for FET measurements, thermal denaturation curves were obtained under various conditions (Table II). Note that if FET experiments are carried out at or below 10 °C, both the junction and the linear duplex are completely annealed. Stable formation of the 10 bp/arm four-way junction was also confirmed by gel electrophoresis (data not shown), in a manner analogous to that described previously (Kallenbach et al., 1983; Cooper & Hagerman, 1987). In particular, only the two-strand combinations that would be expected to anneal along half their lengths (due to partial sequence complementarity) produce bands that migrate more slowly than the component single strands. Moreover, the four-strand complex runs as a discrete band.

Measurement of FET between the Ends of an Oligonucleotide Duplex. The fluorescent dyes fluorescein and eosin were used as the donor–acceptor pair for most of the FET experiments. Eosin excitation is well resolved from fluorescein excitation and occurs within the fluorescein emission range; thus, the spectral overlap of the two dyes is well suited for measurements of donor quenching. For those measurements, samples were excited at the wavelength of maximum donor excitation (496 nm), and emission was monitored over the range of donor emission (508–540 nm). A typical FET determination involved measurement of the fluorescence emission of four samples: donor-linked single strand (D); donor-linked strand annealed to its unlabeled, complementary strand (DU); donor-linked strand and acceptor-linked complement (DA); unlabeled donor strand and acceptor-linked complement (AU). The concentrations of donor and acceptor strands were held constant in all four samples. In order to ensure that each donor-linked duplex contained an acceptor strand, DU, DA, and AU samples contained a molar excess of acceptor strand. Since the precise extinction coefficients of the fluorophore-linked oligonucleotides were not determined, the required ratio of acceptor-linked to donor-linked strands was determined empirically by adding increasing amounts of acceptor-linked strand to a constant quantity of donor-linked strand. Apparent transfer efficiencies (E_{app}) reached plateau values when an approximately 2–5-fold molar excess of acceptor-linked strand (as estimated by ultraviolet absorbance at 260 nm) was employed; therefore, a 4–5-fold molar excess of acceptor strand was used throughout this study.

An example of the emission spectra obtained from a set of measurements is shown in Figure 1. In order to determine E_{app}, the following operations were carried out: (i) the fluorescence emission due to direct excitation of the acceptor (curve AU) was subtracted from the emission of donor in the presence of acceptor (curve DA), (ii) the ratio of the integral (over an approximately 10-nm range spanning the donor emission maximum) of the resulting curve (DA–AU) to that of the curve representing donor fluorescence in the presence

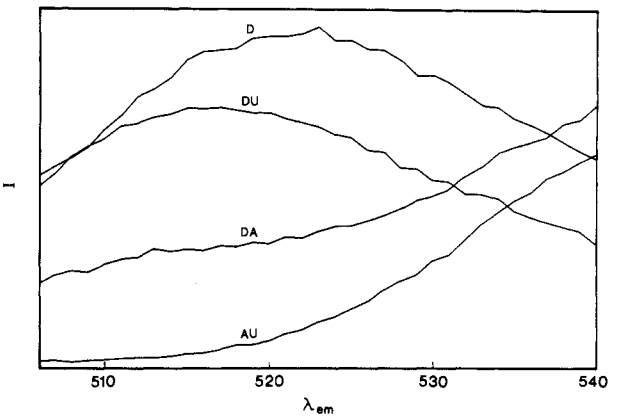

FIGURE 1: Spectra obtained for a typical FET measurement. The relative fluorescence intensity, *I*, is plotted versus emission wavelength (nm) for the 11-mer, with fluorescein as donor fluorophore and eosin as acceptor fluorophore. Curves D, DU, DA, and AU are described in the text. Solution compositions: 36 nM donor strand, 140 nM acceptor strand, 40 mM Tris acetate, 20 mM sodium acetate, 1 mM EDTA, 5 mM magnesium acetate, pH 7.9.

of unlabeled complement (curve DU) was determined, and (iii) the apparent efficiency (E_{app}) of FET was obtained from the relation $E_{app} = 1 - [\int(DA - AU)/\int DU]$. From the spectra shown in Figure 1, obtained from measurements of FET between the ends of an 11-mer, $E_{app} = 0.61$. Figure 1 also illustrates a phenomenon that was observed for all of the linear duplexes studied: donor fluorescence intensity changes upon hybridization of the donor-linked strand to its unlabeled complement (compare curves D and DU); in addition, the wavelength of maximum donor emission shifts upon the formation of duplex DNA. The implications of this potentially significant effect will be considered below.

In order to establish that FET occurs only within individual duplexes, donor emission was measured in samples in which donor and acceptor fluorophores were attached to noncomplementary oligonucleotide strands [i.e., donor and acceptor fluorophores both attached to separate molecules of the same single-strand sequence (11-mer, Table I)]. In this control experiment, donor emission was unaffected by the presence of acceptor.

FET Measurements of a Series of Duplexes of Varying Length. The quantitation of distances from FET data generally relies on the theory developed by Forster (1948), in which FET occurs through a dipole–dipole coupling mechanism; Forster determined that the efficiency of the transfer process should depend on the inverse sixth power of the distance between fluorophores. In order to ascertain whether the Forster mechanism holds for transfer between fluorophores that are attached to DNA molecules, a series of FET experiments was carried out on duplexes of varying length. The sequences of the oligonucleotides that were studied are enumerated in Table I. Each *n*-mer duplex contained *n* bp,

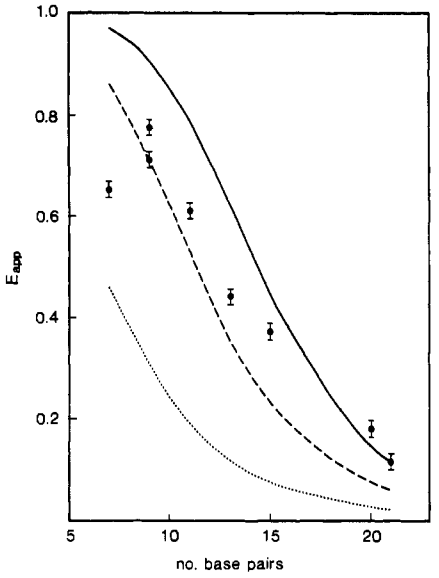

FIGURE 2: FET data points and Forster curves for an R_0 value of 55 Å. The E_{app} values listed in Table III are plotted along with computed Forster curves for three tether lengths: 5-Å tether (continuous line); 10-Å tether (dashed line); 18-Å tether (dotted line). The Forster curves were computed from the equation $E = 1/[1 + (R/R_0)^6]$, with R_0 = 55 Å and $R = [3.4\text{Å}(n - 1) + 2(\text{tether length})]$, where n = number of base pairs.

comprising $n - 1$ paired bases and an unpaired thymidine residue at each 5′-end. The 5′-thymidine overhangs were added to reduce the potential for terminal stacking of the fluorophores on the helices; such stacking interactions might modify the transfer efficiencies, either by restricting the angular motions of the probes or by increasing the probability of through-helix transfer.

The measured E_{app} values for each duplex are listed in Table III and presented graphically in Figure 2. The effective length of the duplex DNA-to-fluorophore tether [which comprises 5′-phosphate of duplex – thymidine residue – phosphate – $(CH_2)_2NH$ – fluorophore] is unknown; however, distance computations (kindly performed by Karl Hahn using the program ALCHEMY) indicate that the maximum length of the fully extended tether, with no base stacking interactions between the unpaired thymidine residues and the duplexes, would be 18 Å. Therefore, expected FET efficiencies (based on the Forster equation with an R_0 value of 55 Å; see Materials and Methods) are also plotted for an extreme range of possible tether lengths (≤18 Å).

Inspection of Figure 2 reveals that, while there is a clear dependence of E_{app} on the number of nucleotides in the molecule, the E_{app} values decrease less rapidly with increasing oligomer length than expected for simple Forster transfer. One possible source of this apparent discrepancy is the use of an R_0 value of 55 Å, which reflects the standard assumption of complete orientational freedom of both donor and acceptor fluorophores ($\kappa^2 = {}^2/_3$). Assigning a large value for tether length (which would compensate for the lack of a sufficiently steep variation in E_{app} by reducing the percentage change in fluorophore separation represented by a given range of molecular lengths), while allowing R_0 to float to larger values, results in better correspondence between the experimental and computed curves (see Figure 3). Implicit in a larger R_0 value is a κ^2 value considerably larger than two-thirds. Indeed, applying the analysis of Dale et al. (1979), our polarization experiments indicate that the fluorophores may not experience complete motional freedom (donor axial depolarization factor 0.62, acceptor axial depolarization factor 0.79–0.88); thus κ^2 may vary between ~0.2 and 2.6, leading to R_0 values ranging from 45 to 70 Å. However, given the expected rotational freedom about a fully extended tether, it is unlikely that the motions of the fluorophores would be highly restricted. On the contrary, anisotropy of donor and acceptor dipole orientations suggests that interactions are occurring between the probes and the DNA helix; such interactions imply a short effective tether length, a situation that cannot yield congruence between the data and the Forster equation.

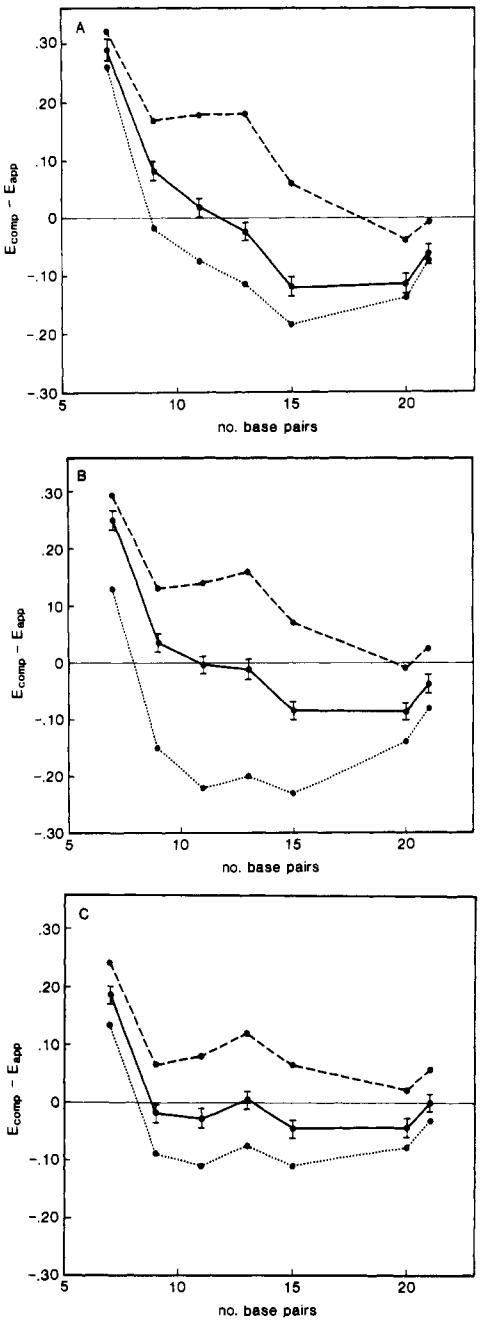

FIGURE 3: Divergence between Forster curves and experimental curves. The differences between FET efficiencies calculated from the Forster equation and experimental E_{app} values, $E_{comp} - E_{app}$, are plotted versus number of base pairs. (A) Difference plots are shown for a tether length of 5 Å, with three R_0 values: R_0 45 Å (dotted line); R_0 = 48 Å (continuous line); R_0 = 55 Å (dashed line). (B) Difference plots for a tether length of 10 Å: R_0 = 50 Å (dotted line); R_0 = 58 Å (continuous line); R_0 = 65 Å (dashed line). (C) Difference plots for tether length of 18 Å: R_0 = 70 Å (dotted line); R_0 = 74 Å (continuous line); R_0 = 80 Å (dashed line). In each panel, error bars are shown only on the curves representing the R_0 value that yields the best correspondence between computed (Forster) curves and data curves for a given tether length.

Table III: FET Efficiencies for Oligonucleotide Duplexes[a]

species	E_{app}[b,c]	species	E_{app}[b,c]
7-mer	0.65	13-mer	0.44
9-mer(a)	0.78	15-mer	0.37
9-mer(b)	0.71	20-mer	0.18
11-mer	0.61	21-mer	0.12

[a] Solution compositions: 36 nM donor strand, 140 nM acceptor strand, 40 mM Tris acetate, 20 mM sodium acetate, 1 mM NaEDTA, 5 mM magnesium acetate, pH 7.9; temperature, 5 °C. [b] Measured efficiency of FET between fluorescein (donor) and eosin (acceptor) moieties at either end of the molecule, calculated from the integrated emission intensities of DU, DA, and AU curves as described in the text. [c] Each E_{app} value represents the average of at least two measurements. The sample standard deviation associated with E_{app}, $S(E_{app})$, obtained from six independent measurements of FET between the ends of 9-mer(b), was 0.017; this value for $S(E_{app})$ is represented in Figures 4 and 5 as a vertical bar and was used in calculations of variance ratios. The observed $S(E_{app})$ values for species other than 9-mer(b) were all less than 0.017.

An analysis of variance ratios (see Methods) indicates that for all possible values of tether length (≤18 Å), irrespective of R_0, the differences between experimental and Forster curves are significant at a level of 0.005 (data not shown). Exclusion of the 7-mer data point results in closer agreement between the data and Forster curves, particularly for tether lengths ≥14 Å with R_0 values ≥67 Å. However, two considerations justify the inclusion of the 7-mer data point: (1) there is no a priori reason for its exclusion and (2) UV melting curves show that the 7-mer is annealed under the experimental conditions used for FET (Table II).

It should also be noted that the predicted E_{app} values do not take into account the relative positions, on the surface of the cylinder outlined by the helix, of the points of attachment of the two tethers. This latter effect has been considered in a series of distance computations (P. J. Hagerman, unpublished data). Although the computed distances deviate, as expected, from those obtained by simply assuming a duplex distance of 3.4 Å/bp, the deviations are relatively small and cannot account for the FET data as analyzed by using the Forster equation.

In addition, the current analysis has not considered explicitly the translational freedom of the probes at the ends of the tethers (Amir & Haas, 1986; Lakowicz et al., 1988; Gryczynski et al., 1988; Beechem & Haas, 1989). However, such motions would tend to weight the apparent tether extensions toward smaller effective lengths, a situation that is not supported by the data.

Therefore, in order to interpret our data solely in terms of the Forster equation, one would have to propose (i) that exclusion of the E_{app} value observed for the 7-mer is valid and (ii) that the tethers are almost fully extended, with rigidly attached fluorophores. There is as yet neither evidence nor a tenable physical rationalization in support of either of the above proposals. The inequality (within our limits of experimental error) in E_{app} for two duplexes containing the same number of bases but different sequences [9-mer(a) and 9-mer(b)] further suggests that factors in addition to Forster transfer (e.g., differential dye–helix interactions) influence donor fluorescence. Moreover, sequence-dependent differences in the polarizability of the helix may lead to different R_0 values for the fluorescein/eosin pair among the duplexes studied.

Investigation of Potential Nondipolar Effects on FET. An alternative view of the anomalies in the FET data stems from two related observations: first, both the intensity and wavelength maximum of (oligonucleotide-linked) donor fluorescence differ in the presence and absence of unlabeled, complementary strand (e.g., Figure 1); and second, the magnitude and direction of these fluorescence shifts vary with base sequence (data not shown). In order to further investigate the potential modulation of donor fluorescence by the helical state of the DNA, the fluorescence intensities of several samples were monitored as a function of temperature. Figure 4 shows the fluorescence melting curves for two 9-mers, along with the corresponding curve for free fluorescein; it is clear that the intensity of donor fluorescence changes with the extent of DNA melting. Furthermore, the differences between the fluorescence patterns observed for fluorescein alone and attached to a single oligonucleotide strand (D curves) are strongly indicative of dye–DNA interactions, again implying that the tethers are not fully extended. The striking dependence of this effect on base sequence is also illustrated in Figure 4. Interestingly, changes in fluorescence occur over a temperature range in which absorbance remains constant (Table 2); it is therefore likely that fluorescence measurements detect thermally induced shifts in duplex structure that are not detectable by UV absorbance measurements. Thus, these sequence-dependent phenomena indicate that some mechanism(s) other than dipolar energy transfer affects donor fluorescence in the absence of acceptor at the end of the complementary strand, i.e., that non-Forster mechanisms contribute to donor quenching both in the presence and absence of acceptor. Whether these alternative mechanisms affect donor fluorescence to the same extent in DU and DA samples is a critical issue and is as yet unresolved.

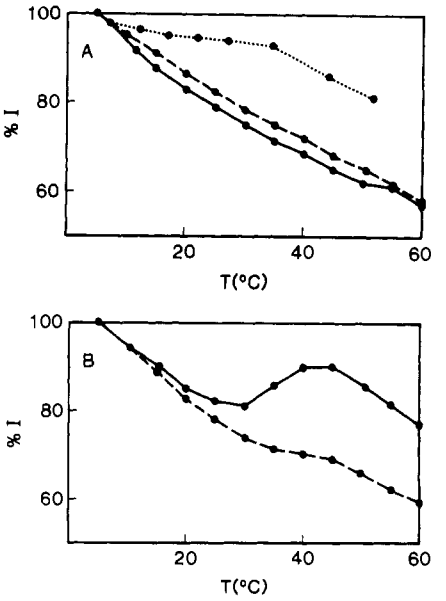

FIGURE 4: Fluorescence melting curves for two 9-mer sequences. The thermally induced changes in fluorescence are plotted as *%I*, the fraction of the highest emission intensity measured at 518 nm. (A) The fluorescence melting curves for D samples (i.e., samples containing a single, fluorescein-linked strand) are shown: 9-mer(a) (continuous line); 9-mer(b) (dashed line); free fluorescein isothiocyanate (approximately 180 nM, dotted line). (B) Fluorescence melting curves for DU samples (i.e., samples containing a fluorescein-linked strand with the unlabeled complementary strand): 9-mer(a) (continuous line); 9-mer(b) (dashed line). Sample compositions: 36 nM fluorescein-linked strand; 140 nM unlabeled complementary strand (in the DU samples); 40 mM Tris acetate; 20 mM sodium acetate; 1 mM NaEDTA; 5 mM magnesium acetate; pH 7.9.

Two preliminary observations may provide further information as to the occurrence of any putative non-Forster transfer mechanisms. First, FET was evaluated by measuring increases in acceptor excitation. The E_{app} values thus derived differ markedly from those obtained via donor quenching measurements (data not shown). Inequalities between FET efficiencies derived from donor quenching and acceptor sen-

sitization have been noted by others (Conrad & Brand, 1968; Berman et al., 1980) and have been attributed to nondipolar quenching mechanisms. Second, in order to determine whether discrepancies between computed and experimental transfer efficiencies are peculiar to the fluorescein–eosin dye pair, FET experiments were performed by using an alternative acceptor fluorophore, tetramethylrhodamine. The fluorescein–tetramethylrhodamine pair has recently been used by others in FET experiments on oligonucleotides (Cardullo et al.; 1988; Murchie et al., 1989). The results of measurements on two duplexes (E_{app} for the 13-mer = 0.48; E_{app} for the 21-mer = 0.17) suggest that the range of E_{app} values for the fluorescein–tetramethylrhodamine pair is similar to that obtained for the fluorescein–eosin pair, implying non-Forster behavior. As is the case for fluorescein, the intensity of (oligonucleotide-linked) eosin fluorescence is changed upon hybridization with an unlabeled complementary strand; the phenomenon is also observed for tetramethylrhodamine-linked strands in the presence and absence of unlabeled complement.

Recently, Cardullo et al. (1988) have reported FET experiments of the type described above, using fluorescein and tetramethylrhodamine as fluorescence donor and acceptor, respectively. Those authors formulated a model for the fluorescent DNA helix based on the distances they calculated from the Forster equation, using experimentally determined E values for three duplexes (an 8-mer, a 12-mer, and a 16-mer). They interpreted their results by assuming that FET between fluorescein and tetramethylrhodamine, placed at either end of a DNA double helix, occurs solely through the Forster mechanism. However, the results of the current study raise two points of potential concern about the study of Cardullo et al. (1988). First, those authors reported a change in donor fluorescence accompanying hybridization to unlabeled complement (reduced by 26%) for each of the duplexes studied. This observation is consistent with our own results in that changes in donor fluorescence occur in the absence of acceptor and suggests that non-Forster effects may be operating. Second, Cardullo et al. (1988) observed the same efficiency for transfer between the free ends flanking a four-nucleotide single-strand gap as that which they observed for the 8-mer, suggesting that E_{app} is not, in fact, strictly related to the inverse sixth power of R in their experiments.

FET between the Ends of the Arms of the DNA Four-Way Junction. Synthetic DNA four-way junctions have been used as stable models for branched recombination intermediates (Kallenbach et al., 1983; Mueller et al., 1988; Cooper & Hagerman, 1989, and references therein). Since the higher order structures of such intermediates may influence the outcome of genetic recombination, there has been considerable interest in elucidating the geometries of the synthetic junctions. The results of FET measurements between fluorescein and eosin attached to each possible pair of arms of the DNA four-way junction are presented in Table IV. While the relative angles obtained by analyzing the FET data with the Forster equation agree qualitatively with those obtained by other methods (Cooper & Hagerman, 1987, 1989), the apparent angles (based on FET measurements) for the less bent pairs of junction arms (1/2, 1/3, 2/4, and 3/4) are considerably more acute than the corresponding angles determined from the birefringence experiment. One possible explanation of the FET data might invoke a large degree of flexibility of the junction core. The angles in Table IV are calculated by using the Forster equation, with E_{app} proportional to R^{-6}; therefore, if the angles between junction arms were constantly changing (about certain minimum energy values), the junction

Table IV: Apparent FET Efficiencies and Corresponding Distances for the DNA Four-Way Junction

dye-labeled junction arms[a,b]	E_{app}	range of distances (Å)[c]	range of angles[d] (deg)
1D/2A	0.31	55–85	90–109
2D/1A	0.27	57–87	94–113
1D/3A	0.25	58–89	96–118
3D/1A	0.27	57–87	94–113
1D/4A	0.61	45–69	70–83
4D/1A	0.44	50–77	80–95
2D/3A	0.46	49–76	78–94
3D/2A	0.59	45–70	70–85
2D/4A	0.24	58–90	96–120
4D/2A	0.30	55–85	90–110
3D/4A	0.24	58–90	96–120
4D/3A	0.23	59–91	98–121

[a] Sample compositions: 340 nM donor strand, 1.4 μM acceptor strand, 10 mM Tris-HCl, 5 mM $MgCl_2$, pH 8.0. [b] Numbers refer to the junction arms so named in Table I and in previous work (Cooper & Hagerman, 1987, 1989). D indicates the fluorescein-linked strand; A indicates the eosin-linked strand. [c] Distances were calculated from the equation $R = R_0[(1 - E_{app})/E_{app}]^{1/6}$; the low end of the distance range was derived from R_0 = 48 Å (48 Å being the R_0 value that yields the best correspondence between the data and the Forster equation for a tether length of 5 Å), the high end from R_0 = 74Å (the R_0 value yielding best fit for a tether length of 18 Å). [d] Range of (included) angles between the dye-linked junction arms calculated from the equation, angle = $2[\sin^{-1}(R/2xl)]$ where l = length of the junction arm (in Å). For the low end of range of angles, l = 39 Å [(10 bp × 3.4 Å/bp) + 5-Å tether]; for the high end of range, l = 52 Å (18-Å tether).

configuration with the fluorophores at closest approach would contribute most to the observed transfer efficiencies. However, in previous work (Cooper & Hagerman, 1989), we have ruled out a point of significant increased flexibility at the junction core (in the presence of magnesium).

If factors in addition to dipolar FET are operative in the experiments on junctions, such effects must be quantified before FET can be used to determine the interarm angles. It is conceivable that any non-Forster mechanisms that involve energy transfer through the DNA helix would be less significant in the junction, in which FET can presumably occur through free solution as well. However, the observation that transfer efficiencies are changed by interconverting the positions of donor and acceptor (e.g., for 2D/3A, E_{app} = 0.46, while for 3D/2A, E_{app} = 0.59; see Table IV) suggests sequence-dependent effects similar to those observed for the linear duplexes. Thus, alternative mechanisms of energy transfer and/or dissipation may be present in the junction experiment as well; this supposition is further supported by the lack of the expected variation in the deduced interarm angles.

Murchie et al. (1989) have recently reported a FET analysis of two DNA four-way junctions. Whether the conclusions drawn from that study are valid can be determined only after performing the following control experiments: (1) The assumption that junctions of any sequence adopt a planar-tetragonal geometry in the absence of magnesium must be independently verified. That assumption certainly does not apply to the junction studied in the current work (Cooper & Hagerman, 1987, 1989). (2) The assumed relationship between FET efficiency and the distance between fluorophores must be confirmed experimentally. This latter issue is particularly important since interactions between the dyes and the ends of their junction arms were noted prior to the addition of a 5′-CpC sequence to each junction arm (Murchie et al., 1989); the assumed constancy of dye–duplex interactions among the CpC-derivatized molecules must also be confirmed. (3) The method used by Murchie et al. (1989) for standardizing

samples is only accurate if every junction contains exactly one donor and one acceptor and if donor fluorescence diplays no sequence dependence. Both of these conditions must be demonstrated experimentally. (4) The limits of experimental error must be defined. The importance of this last point is most clearly illustrated by the rhodamine "walking" experiment in which significant conclusions were drawn from a graph with an ordinate scale of 0.103–0.108. Our sample standard deviation of 0.017 (see legend to Table III) would render differences within 0.5% insignificant. Analysis of that experiment must also take account of the length/spacial orientation of the $(CH_2)_6NH$–fluorophore tethers. It is unclear whether any of the above-mentioned control studies were performed.

Conclusions

Taken together, our data suggest that the Forster equation alone does not provide a quantitative description of FET in linear or branched DNA molecules. In particular, the following observations suggest a more complex process: (1) The E_{app} values obtained for a set of oligonucleotide duplexes of varying length cannot be fit to the Forster equation (assuming a single R_0 value for the entire experimental set) without invoking a highly extended fluorophore-to-duplex linker, while somehow still allowing direct interactions of the fluorophores with the duplexes, leading to restricted fluorophore motion. (2) The E_{app} values for the 9-mers and the junction appear to depend on base sequence. (3) Donor fluorescence is extremely sensitive to the duplex state of the oligomer, again in an apparently sequence-dependent fashion. (4) The angles between the arms of a DNA four-way junction, derived from analysis of the FET data by using the Forster equation, do not differ as much as expected on the basis of well-established methods. Therefore, the magnitude, sequence dependence, and dye specificity of any non-Forster transfer mechanisms, as well as any variation in R_0 with sequence, must be systematically explored before distances in DNA (or RNA) molecules can be quantified by using FET.

The apparent efficiencies of FET between the ends of the arms of the DNA four-way junction indicate *relative* junction interarm angles that agree with the rank-ordering of angles obtained from gel electrophoretic and transient electric birefringence studies, thereby confirming those results with a nonhydrodynamic technique that applies to junction structure in free solution. However, we caution that nondipolar transfer effects may be operative in the junction system, thus rendering premature quantitative conclusions regarding junction interarm angles.

Acknowledgments

We are indebted to Dr. Mark Griep for numerous helpful discussions pertaining to the use of the spectrofluorometer and of FET in general. We thank Dr. Charles McHenry for generously making his spectrofluorometer available and for useful discussions. We thank Dr. Greg Dewey for first suggesting that FET might be useful for studies of DNA four-way junctions and for valuable discussions. We thank Janine Mills for her efficient operation of the DNA synthesizer, Drs. Dermot Cooper and Mark Seville for help with HPLC, and Karl Hahn for modeling and distance computations of the fluorophore-DNA tether.

References

Amir, D., & Haas, E. (1986) *Biopolymers 25*, 235–240.

Atkinson, T., & Smith, M. (1984) in *Oligonucleotide Synthesis, A Practical Approach* (Gait, J. J., Ed.) pp 35–81, IRL Press, Oxford.

Beardsley, K., & Cantor, C. R. (1970) *Proc. Natl. Acad. Sci. U.S.A. 65*, 39–46.

Beechem, J. M., & Haas, E. (1989) *Biophys. J. 55*, 1225–1236.

Berman, H. A., Yguerabide, J., & Taylor, P. (1980) *Biochemistry 19*, 2226–2235.

Cardullo, R. A., Agrawal, S., Flores, C., Zamecnik, P. C., & Wolf, D. E. (1988) *Proc. Natl. Acad. Sci. U.S.A. 85*, 8790–8794.

Caruthers, M. H., Beaucage, S. L., Efcavitch, J. W., Fisher, E. F., Goldman, R. A. deHaseth, P. L., Mandecki, W., Matteucci, M. D., Rosendahl, M. S., & Stabinsky, Y. (1982) *Cold Spring Harbor Symp. Quant. Biol. 47*, 411–418.

Conrad, R. H., & Brand, L. (1968) *Biochemistry 7*, 777–787.

Cooper, J. P., & Hagerman, P. J. (1987) *J. Mol. Biol. 198*, 711–719.

Cooper, J. P., & Hagerman, P. J. (1989) *Proc. Natl. Acad. Sci. U.S.A. 86*, 7336–7340.

Dale, R. E., Eisinger, J., & Blumberg, W. E. (1979) *Biophys. J. 26*, 161–194.

Fairclough, R. H., & Cantor, C. R. (1978) *Methods Enzymol. 48*, 347–379.

Forster, T. (1948) *Ann. Phys. (Leipzig) 2*, 55–75.

Gryczynski, I., Wiczk, W., Johnson, M. L., Cheung, H. C., Wang, C.-K., & Lakowicz, J. R. (1988) *Biophys. J. 54*, 577–586.

Holowka, D., & Baird, B. (1983a) *Biochemistry 22*, 3466–3474.

Holowka, D., & Baird, B. (1983b) *Biochemistry 22*, 3475–3484.

Kallenbach, N. R., Ma, R.-I., & Seeman, N. C. (1983) *Nature 305*, 829–831.

Lakowicz, J. R., Gryczynski, I., Cheung, H. C., Wang, C.-K., & Johnson, M. L. (1988) *Biopolymers 27*, 821–830.

Merrington, M., & Thompson, C. M. (1943) *Biometrika 33*, 73–88.

Mueller, J. E., Kemper, B., Cunningham, R. P., Kallenbach, N. R., & Seeman, N. C. (1988) *Proc. Natl. Acad. Sci. U.S.A. 85*, 9441–9445.

Murchie, A. I. H., Clegg, R. M., von Kitzing, E., Duckett, D. R., Diekmann, S., & Lilley, D. M. J. (1989) *Nature 341*, 763–766.

Odom, O. W., Jr., Robbins, D. J., Lynch, J., Dottavio-Martin, D., Kramer, G., & Hardesty, B. (1980) *Biochemistry 19*, 5947–5954.

Robbins, D. J., Odom, O. W., Jr., Lynch, J., Kramer, G., Hardesty, B., Liou, R., & Ofengand, J. (1981) *Biochemistry 20*, 5301–5309.

Smith, L. M., Fung, S., Hunkapiller, M. W., Hunkapiller, T. J., & Hood, L. E. (1985) *Nucleic Acids Res 13*, 2399–2412.

Stryer, L., & Haugland, R. P. (1967) *Proc. Natl. Acad. Sci. U.S.A. 58*, 719–726.

Taylor, D. L., Reidler, J., Spudich, J. A., & Stryer, L. (1981) *J. Cell Biol. 89*, 362–367.

Weber, G., & Teale, F. W. J. (1957) *Trans. Faraday Soc. 53*, 646–655.

Yang, C.-H., & Soll, D. (1974) *Proc. Natl. Acad. Sci. U.S.A. 71*, 2838–2842.